UC Davis
UC Davis Previously Published Works

Title
Geothermal energy and ore-forming potential of 600 °C mid-ocean-ridge hydrothermal fluids

Permalink
https://escholarship.org/uc/item/4n78s2vw

Journal
Geology, 48(12)

ISSN
0091-7613

Authors
Bali, Enikő
Aradi, László E
Zierenberg, Robert
et al.

Geothermal energy and ore-forming potential of 600 °C mid-ocean-ridge hydrothermal fluids

Enikő Bali[1]*, László E. Aradi[2], Robert Zierenberg[3], Larryn W. Diamond[4], Thomas Pettke[4], Ábel Szabó[2],
Guðmundur H. Guðfinnsson[1], Guðmundur Ó. Friðleifsson[5] and Csaba Szabó[2]
[1]Nordic Volcanological Center, Institute of Earth Sciences, University of Iceland, Sturlugata 7, 101 Reykjavík, Iceland
[2]Lithosphere Fluid Research Laboratory, Institute of Geography and Earth Sciences, Eötvös University, Pázmány p. sétány 1/C,
 1117 Budapest, Hungary
[3]Earth and Planetary Sciences, University of California–Davis, One Shields Avenue, Davis, California 95616, USA
[4]Institute of Geological Sciences, University of Bern, Baltzerstrasse 3, 3012 Bern, Switzerland
[5]Iceland Deep Drilling Project (IDDP) Office, Vidilundur 10, 210 Gardabaer, Iceland

ABSTRACT

The ~4500-m-deep Iceland Deep Drilling Project (IDDP) borehole IDDP-2 in Iceland penetrated the root of an active seawater-recharged hydrothermal system below the Mid-Atlantic Ridge. As direct sampling of pristine free fluid was impossible, we used fluid inclusions to constrain the *in situ* conditions and fluid composition at the bottom of the hydrothermal convection cell. The fluid temperature is ~600 °C, and its pressure is near-hydrostatic (~45 MPa). The fluid exists as two separate phases: an H_2O-rich vapor (with an enthalpy of ~59.4 kJ/mol) and an Fe-K–rich brine containing 2000 µg/g Cu, 3.5 µg/g Ag, 1.4 µg/g U, and 0.14 µg/g Au. Occasionally, the fluid inclusions coexist with rhyolite melt inclusions. These findings indicate that the borehole intersected high-energy steam, which is valuable for energy production, and discovered a potentially ore-forming brine. We suggest that similar fluids circulate deep beneath mid-ocean ridges worldwide and form volcanogenic massive sulfide Cu-Zn-Au-Ag ore deposits.

INTRODUCTION AND GEOLOGICAL BACKGROUND

The Iceland Deep Drilling Project (IDDP) explores the economic potential of geothermal fluids in the deep roots of active geothermal systems (Friðleifsson et al., 2020). This includes evaluation of the feasibility of exploiting supercritical fluid for energy production and/or extracting economically valuable elements directly from this fluid (e.g., Maimoni, 1982; McKibben and Elders, 1985). Model calculations suggest that the power output of such a hot geothermal well can be an order of magnitude higher than from conventional wells (Albertsson et al., 2003), and it is well known that supercritical fluids may transport metals in high quantities (e.g., Loucks and Mavrogenes, 1999; Simon et al., 2006). The IDDP-2 borehole was drilled in 2016–2017 by deepening an earlier

*E-mail: eniko@hi.is

borehole, RN-15, in the Reykjanes geothermal system in southwest Iceland (Fig. 1) to reach a vertical depth of ~4500 m (total slant depth of 4659 m; Friðleifsson et al., 2020). This is the deepest high-temperature geothermal borehole in the world. Drill-core samples recovered from the sheeted dike complex of this active spreading center also provide a window into processes operating deep beneath the Mid-Atlantic Ridge. At ~4500 m depth, the metabasalt and metagabbro show hydrothermal alteration to amphibole-plagioclase-clinopyroxene-orthopyroxene at temperatures from 700 °C to >900 °C, with median temperatures of ~800 °C (Friðleifsson et al., 2020; Zierenberg et al., 2021). Paragenetically later alteration assemblages record continuing alteration down to 600 °C in the latest-stage, crosscutting veins (Zierenberg et al., 2021).

The major-element composition of geothermal fluid recovered from shallower depths

(<3000 m) in other boreholes is close to that of seawater (Arnórsson, 1978), with trace-metal contents somewhat higher than those typical of black smokers (Hannington et al., 2016), which produce volcanogenic massive sulfide ore deposits on and beneath the ocean floor. This study focused on the examination of fluid inclusions (small droplets of geothermal fluid trapped in minerals) in paragenetically late-stage plagiogranite veins (Zierenberg et al., 2021; see also the Supplemental Material[1] and Figs. S1a and S1b therein) from the bottom part of the borehole (4630–4640 m) in order to determine the physical state, temperature, and composition of the fluid circulating in the rock pores at this depth beneath mid-ocean ridges.

METHODS

We identified phases within the fluid inclusions by optical microscopy and Raman spectroscopy (at room and at high temperature), and by a focused ion beam–scanning electron microscopy slice-and-view technique coupled with energy-dispersive spectrometry (FIB-SEM-EDS). The temperature of the vapor-rich and brine fluids at the time of trapping was determined by heating experiments using Linkam TMS600 and Linkam TS1500 heating stages combined with Raman spectroscopy. These analyses were carried out at the Research and Instrument Core Facility (RICF) of the Faculty of Science at Eötvös University, Budapest, Hungary. Petrographic studies were complemented by cathodoluminescence imaging to confirm the secondary timing of the

---

PETROGRAPHY AND FLUID COMPOSITIONS

The studied plagiogranite veins consist of intermediate plagioclase with minor quartz, apatite, biotite, and Fe-Ti oxides. Groups of coeval fluid inclusions (i.e., fluid inclusion assemblages [FIAs]) were identified in plagioclase and quartz. Inclusions trapped during growth of the host minerals (i.e., primary inclusions) occur as FIAs along the outermost rims of individual crystals and might be coeval with the last stage of plagiogranite vein formation. In contrast, inclusions trapped after vein formation (i.e., secondary inclusions) are represented by FIAs within healed cracks (Fig. 2A) that cut grain boundaries. This study focused on the secondary FIAs, because these represent *in situ* samples of the actively circulating geothermal fluid.

Three compositional types of inclusions occur in the secondary FIAs (see the Supplemental Material). Vapor-rich inclusions (Fig. 2B; Figs. S2a and S4) are dominated by H_2O vapor with minor CO_2, H_2S, and traces of H_2 (determined based on Dubessy et al. [1989]; see also Table S1). Trace-element analyses of individual fluid inclusions showed that values of Cl/Br, B/Cl, and S/Cl in vapor-rich inclusions are comparable to those in seawater, within analytical uncertainty. However, these inclusions are enriched in base and noble metals, but depleted in halogens, B, S, and Mg, relative

studied inclusions. Analyses of minerals and melt inclusions were carried out using a JEOL JXA-8230 SuperProbe at the Institute of Earth Sciences, University of Iceland (Reykjavík). Concentrations of 28 elements in individual fluid inclusions were determined by laser-abla-

tion–inductively coupled plasma–mass spectrometry (LA-ICP-MS) at the University of Bern (Switzerland) employing the procedures of Pettke et al. (2012). A detailed description of the analytical methods is provided in the Supplemental Material.
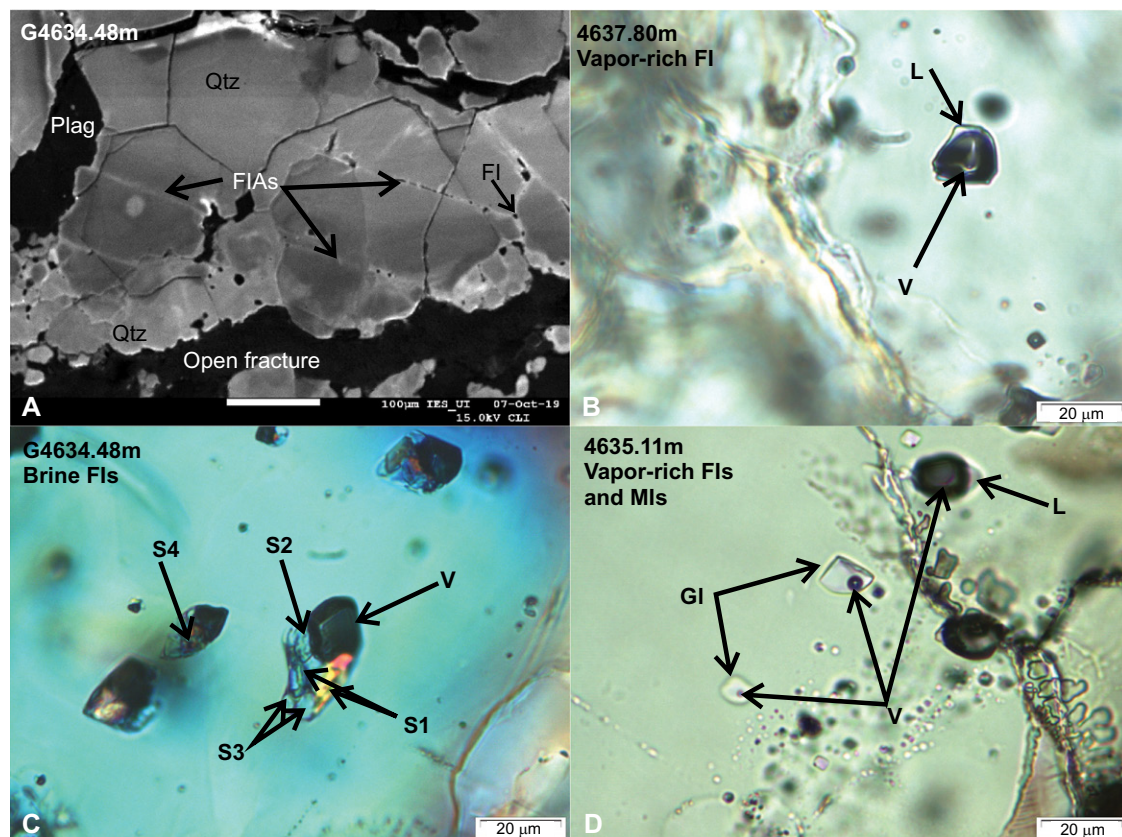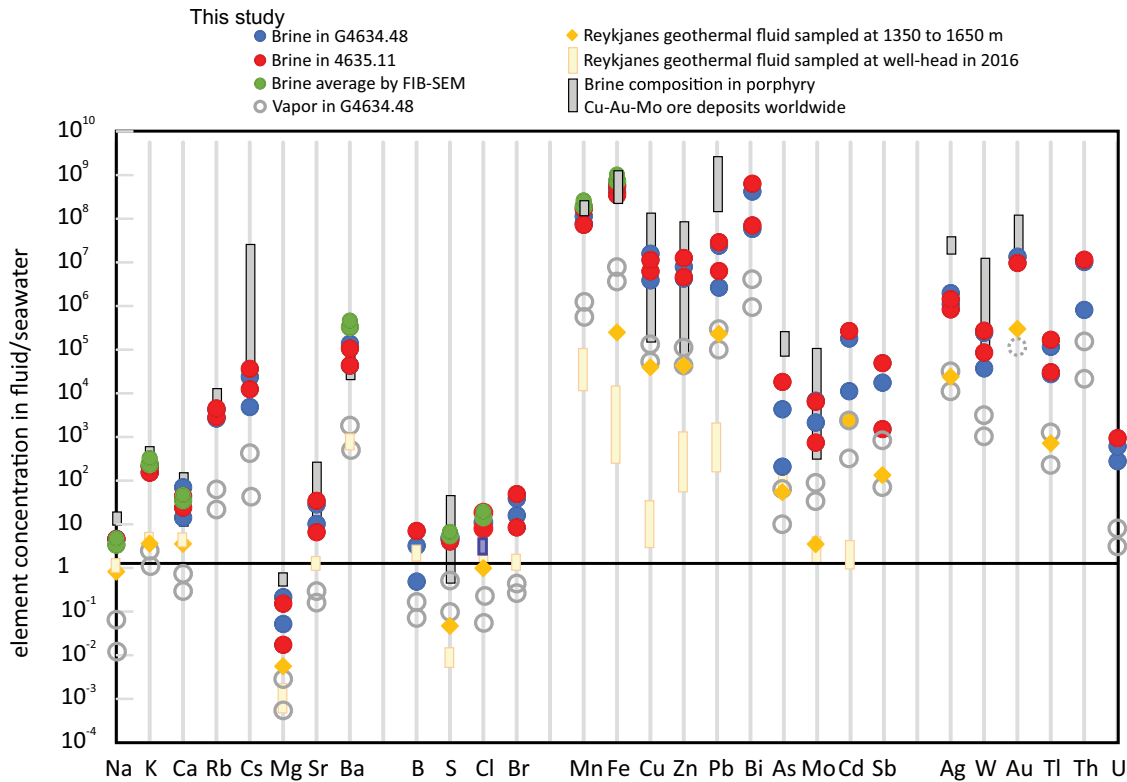
Figure 3. Major- and trace-element compositions of geothermal fluid at 4500 m depth measured in fluid inclusions from Iceland Deep Drilling Project (IDDP) borehole IDDP-2 in southwest Iceland, normalized to seawater (Li, 1991). Pairs of symbols with same color for given element indicate mean value ±2σ standard deviations, as calculated from all measurements of given element in respective inclusion type. In vapor phase, Au is below detection limit, as indicated by dotted circle. Compositions of the Reykjanes geothermal fluid sampled at 1350–1650 m depth (Hannington et al., 2016) and at the well head (Óskarsson and Galeczka, 2017) in other boreholes are shown for comparison. We also plot compilation of fluid inclusion compositions in hypersaline brine inclusions from porphyry ore deposits (Audétat et al., 2008; Rottier et al., 2016; Mernagh and Mavrogenes, 2019). FIB-SEM—focused ion beam–scanning electron microscopy.

to seawater (Fig. 3; Li, 1991). Brine inclusions are composed of four optically distinguishable solids, including halite (Figs. S2b and S3; Table S1), and a vapor bubble ± minor liquid phase (Fig. 2C; Figs. S2b and S3). The proportion of vapor varies within individual FIAs between 20 and 40 vol%. Brine inclusions contain 9–15 wt% Fe, 6–8.5 wt% K, 15–35 wt% Cl, and ~5 wt% Na (Table S1). Although the absolute concentrations of halogens (Cl, Br) are an order of magnitude higher in the brine inclusions, their ratio is similar to that in seawater (Li, 1991). The third inclusion type is trapped silicate melt (Fig. 2D), which is composed of colorless rhyolitic silicate glass and a vapor bubble. These inclusions only occasionally coexist with the vapor-rich and brine inclusions (Figs. S2d–S2f; Table S3).

IMPLICATIONS
Determination of *In Situ* Conditions

The variable proportions of the three inclusion types within the same secondary FIAs could in principle reflect initial entrapment of a single-phase fluid that underwent phase separation during continued fracture healing. However, the spatial distribution of the vapor-rich and brine inclusions rules out such an origin via necking down (Roedder, 1984). Rather, the textures (Fig. 2; Fig. S2) show that two and occasionally three immiscible fluids were trapped simultaneously within individual fractures upon healing: vapor-rich and brine end members, sometimes

with melt inclusions. Such multiphase entrapment is common in hydrothermal systems (e.g., Audétat et al., 2008; Kodera et al., 2014; Rottier et al., 2016; Mernagh and Mavrogenes, 2019), as verified by experimental studies (Bodnar et al., 1985) and by observations of fluid inclusions in boiling geothermal systems (e.g., Belkin et al., 1985). The variation in vapor:solid proportions in the secondary FIAs is therefore ascribed to accidental physical mixing between the vapor-rich and brine end member fluids prior to inclusion sealing.

In a multiphase fluid system, inclusions that trap only one of the end member phases will homogenize at the temperature of trapping (Roedder, 1984). Homogenization should occur into the vapor phase in one end member at the same temperature as the other end member homogenizes into the liquid phase. In our samples, *in situ* Raman spectroscopy showed that the vapor-rich inclusions homogenized at 600 ± 20 °C (see the Supplemental Material), which we interpret as the trapping temperature of the immiscible fluids at ~4500 m depth. In the brine inclusions, halite dissolves at 377–390 °C, which rules out the presence of halite during fluid entrapment, but the accompanying Cu-Fe sulfide dissolves at 600 ± 20 °C, suggesting that the fluid was saturated in this phase during trapping. This is confirmed by the presence of interstitial Cu-Fe–sulfide minerals both in the altered metabasalt (Zierenberg et al., 2021) and

in the felsic veins (see the Supplemental Material; Fig. S1b). However, the brine inclusions do not homogenize completely to liquid at this temperature because they contain various amounts of accidentally trapped vapor end member.

We can derive a first-order approximation of the conditions of the phase transitions in coexisting vapor and hypersaline brine inclusions by considering the phase behavior in the binary $NaCl-H_2O$ system (Driesner, 2007). Based on the observed halite dissolution temperatures of 377–390 °C, the coexisting vapor should homogenize between 595 °C and 597 °C, if these fluid inclusions were simultaneously trapped in their host minerals at pressures between 50 and 60 MPa (Driesner, 2007). The presence of $FeCl_2$ in a saline fluid, however, changes the position of the critical curve in pressure-temperature-composition (*P-T-X*) space. Because the critical curve in the $FeCl_2-H_2O$ system has a lower *dP/dT* slope compared to that in the $NaCl-H_2O$ or $KCl-H_2O$ systems (Driesner, 2007; Steele-MacInnis et al., 2015; Shmulovich et al., 1995), the entrapment pressure of the studied fluid inclusions might be slightly lower than the estimated value based on pure $NaCl-H_2O$. Thus, we suggest that the fluid entrapment pressure was close to cold hydrostatic conditions (45 MPa), i.e., somewhat higher than the transient pressure measured near the bottom of the borehole during drilling (Fig. 4; Friðleifsson et al., 2020). At these conditions, the enthalpy of the H_2O-rich
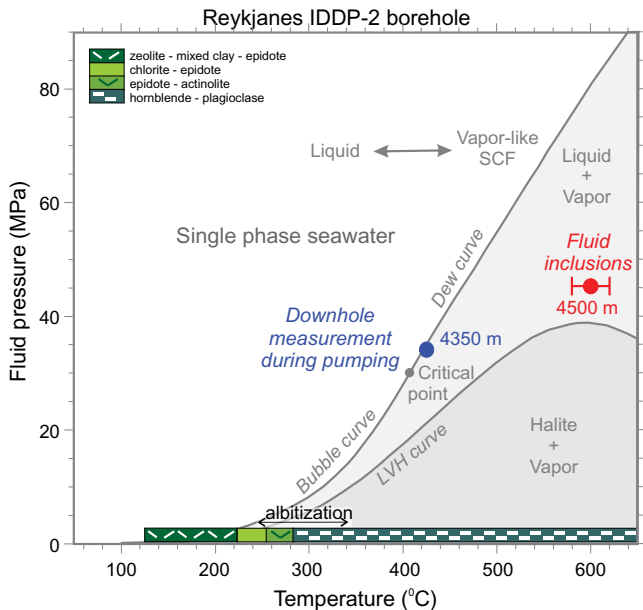
Figure 4. Pressure-temperature (*P-T*) phase relations of NaCl fluids with seawater salinity, based on Driesner (2007). Fluid inclusions formed during late-stage alteration are interpreted to record *in situ* conditions at ~600 °C and 45 MPa, i.e., approximate hydrostatic pressure at 4500 m. Fluids entering the drill hole were measured at 426 °C and 35 MPa, i.e., pressure imposed by pumping rate and cold-water head in the bore hole during measurement (Friðleifsson et al., 2020). Alteration mineralogy as function of *T* in the Reykjanes (Iceland) basaltic crust is based on Zierenberg et al. (2021) and Marks et al. (2010). SCF—supercritical fluid, LVH—liquid-vapor-halite; IDDP-2—Iceland Deep Drilling Project 2.

than conventional geothermal wells, but it also probed a potential ore-forming fluid, similar to those that form volcanogenic massive sulfide deposits on the seafloor.

vapor is estimated to be 59.4 kJ/mol or 3300 kJ/kg (Driesner, 2007), which is two to three times higher than in the currently exploited part of the reservoir (Friðleifsson et al., 2020). At 600 °C and 45 MPa, seawater is unstable as a single fluid but instead exists as low-salinity vapor in equilibrium with a small fraction of hypersaline brine (Fig. 4).

Are the K-Na-Fe-Cl – rich fluid compositions representative of the current state of the hydrothermal system at 4500 m depth? We note that a K-Na-Fe-Cl brine is also present in pores in the drill cores from the bottom of the borehole, as indicated by EDS analyses of yellow salt crystals (K, Fe Cl) and halite crystals precipitated on the surface of cut drill cores following washing and drying of the core (Zierenberg et al., 2021). The lowest temperature recorded by Ti-in-quartz geothermometry on the same samples analyzed for fluid inclusions is also ~600 °C (Zierenberg et al., 2021). Therefore, we suggest that the studied secondary FIAs closely represent the current geothermal fluid.

Interaction of Geothermal Fluid with the Oceanic Crust at ~4500 m Depth

In the shallow part of the Reykjanes geothermal system, the geothermal fluid has a salinity similar to that of seawater, with an Na/K mass ratio of 6.5 (Arnórsson, 1978, 1995). At ~4500 m depth and ~600 °C, the fluid composition is markedly different; here, the fluids have an Na/K mass ratio of 0.7 (Table S1). This change in fluid composition can be attributed to extensive fluid-rock interaction of seawater with the tholeiitic basaltic and gabbroic crust of the Reykjanes Peninsula. Igneous plagioclase is altered to more albitic compositions (Fig. 4; Friðleifsson et al., 2020; Zierenberg et al., 2021;

Marks et al., 2010), depleting the fluid in Na relative to K. Similarly, the replacement of primary igneous clinopyroxene by hornblende (Zierenberg et al., 2021; Marks et al., 2010) leads to a progressive decrease in the Na/K ratio in the geothermal fluid (Fig. 4). These reactions also result in elevated Fe and trace-metal contents in the fluid, whereas the S/Cl, Cl/Br, and halogen/boron ratios remain largely unmodified or are slightly increased (Fig. 3; Table S1).

The contribution of a degassing magmatic fluid from water-undersaturated mid-ocean-ridge basalt is likely to be minor, as it would decrease Cl/B and increase the S/Cl ratio (e.g., Arnórsson, 1995; Lesne et al., 2011; Ármannsson et al., 2014) relative to seawater (see the Supplemental Material for more details). Furthermore, tholeiitic basalts and their fractionation products are sodic. Experimental studies (e.g., Clark, 1966) suggest that, upon fluid separation at crustal conditions, Na partitions more strongly into the brine phase than K. Therefore, tholeiitic silicate melts with Na/K mass ratios above 1 cannot produce a degassing brine with Na/K mass ratio below 1. The high K₂O content of the rhyolite melt inclusions (Table S3) found in association with the fluid inclusions here is atypical for Icelandic rhyolites (Jónasson, 2007). This composition is therefore interpreted to be the result of a reaction with the percolating brine, rather than a primary igneous feature.

The fluid inclusion compositions contain noble and base metals in concentrations similar to those in ~600 °C hot brine inclusions in porphyry-type ore deposits (Fig. 3; e.g., Mernagh and Mavrogenes, 2019, and references therein). This shows that the IDDP-2 borehole not only accessed geothermal fluid that has the potential to produce order-of-magnitude higher energy

REFERENCES CITED
Albertsson, A., Bjarnason, J.Ö., Gunnarsson, T., Ballzus, C., and Ingason, K., 2003, Part III: Fluid handling and evaluation, *in* Fridleifsson, G.Ó., ed., Iceland Deep Drilling Project, Feasibility Report: Reykjavík, Orkustofnun, Report OS-2003-007, p. 2.
Ármannsson, H., Fridriksson, Th., Guðfinnsson, G.H., Ólafsson, M., Óskarsson, F., and Thorbjörsson, D., 2014, IDDP—The chemistry of the IDDP-01 well fluids in relation to the geochemistry of the Krafla geothermal system: Geothermics, v. 49, p. 66–75, https://doi.org/10.1016/j.geothermics.2013.08.005.
Arnórsson, S., 1978, Major element chemistry of the geothermal sea-water at Reykjanes and Svartsengi, Iceland: Mineralogical Magazine, v. 42, p. 209–220, https://doi.org/10.1180/minmag.1978.042.322.07.
Arnórsson, S., 1995, Geothermal systems in Iceland: Structure and conceptual models—I. High temperature areas: Geothermics, v. 24, p. 561–602, https://doi.org/10.1016/0375-6505(95)00025-9.
Audétat, A., Pettke, T., Heinrich, C.A., and Bodnar, R.J., 2008, The composition of magmatic-hydrothermal fluids in barren and mineralized intrusions: Economic Geology and the Bulletin of the Society of Economic Geologists, v. 103, p. 1–32, https://doi.org/10.2113/gsecongeo.103.5.877.
Belkin, H., De Vivo, B., Gianelli, G., and Lattanzi, P., 1985, Fluid inclusions in minerals from the geothermal fields of Tuscany, Italy: Geothermics, v. 14, p. 59–72, https://doi.org/10.1016/0375-6505(85)90094-X.
Bodnar, R.J., Burnham, C.W., and Sterner, S.M., 1985, Synthetic fluid inclusions in natural quartz. III. Determination of phase equilibrium in the system H₂O-NaCl to 1000 °C and 1500 bars: Geochimica et Cosmochimica Acta, v. 49, p. 1861–1873, https://doi.org/10.1016/0016-7037(85)90081-X.
Clark, S.P., 1966, Solubility, *in* Clark, S.P., ed., Handbook of Physical Constants: Geological Society of America Memoir 97, p. 415–436, https://doi.org/10.1130/MEM97-p415.
Driesner, T., 2007, The system H₂O-NaCl. Part II: Correlations for molar volume, enthalpy, and isobaric heat capacity from 0 to 1000 °C, 1 to 5000 bar, and 0 to 1 XNaCl: Geochimica et

Cosmochimica Acta, v. 71, p. 4902–4919, https://doi.org/10.1016/j.gca.2007.05.026.

Dubessy, J., Poty, B., and Ramboz, C., 1989, Advances in C-O-H-N-S fluid geochemistry based on micro-Raman spectrometric analysis of fluid inclusions: European Journal of Mineralogy, v. 1, p. 517–534, https://doi.org/10.1127/ejm/1/4/0517.

Friðleifsson, G.O., et al., 2020, The Iceland Deep Drilling Project at Reykjanes: Drilling into the root zone of a black smoker analog: Journal of Volcanology and Geothermal Research, v. 391, p. 106435, https://doi.org/10.1016/j.jvolgeores.2018.08.013.

Hannington, M., Harðardóttir, V., Garbe-Schönberg, D., and Brown, K.L., 2016, Gold enrichment in active geothermal systems by accumulating colloidal suspensions: Nature Geoscience, v. 9, p. 299–302, https://doi.org/10.1038/ngeo2661.

Jónasson, K., 2007, Silicic volcanism in Iceland: Composition and distribution within the active volcanic zones: Journal of Geodynamics, v. 43, p. 101–117, https://doi.org/10.1016/j.jog.2006.09.004.

Kodera, P., Heinrich, C.A., Wälle, M., and Lexa, J., 2014, Magmatic salt melt and vapor: Extreme fluids forming porphyry gold deposits in shallow sub-volcanic settings: Geology, v. 42, p. 495–498, https://doi.org/10.1130/G35270.1.

Lesne, P., Kohn, S.C., Blundy, J., Witham, F., Botcharnikov, R.E., and Behrens, H., 2011, Experimental simulation of closed-system degassing in the system basalt-H_2O-CO_2-S-Cl: Journal of Petrology, v. 52, p. 1737–1762, https://doi.org/10.1093/petrology/egr027.

Li, Y.H., 1991, Distribution patterns of the elements in the ocean: A synthesis: Geochimica et Cosmochimica Acta, v. 55, p. 3223–3240, https://doi.org/10.1016/0016-7037(91)90485-N.

Loucks, R.R., and Mavrogenes, J.A., 1999, Gold solubility in supercritical hydrothermal brines measured in synthetic fluid inclusions: Science, v. 284, p. 2159–2163, https://doi.org/10.1126/science.284.5423.2159.

Maimoni, A., 1982, Minerals recovery from Salton Sea geothermal brines: A literature review and proposed cementation process: Geothermics, v. 11, p. 239–258, https://doi.org/10.1016/0375-6505(82)90031-1.

Marks, N., Schiffman, P., Zierenberg, R., Franzson, H., and Fridleifsson, G.O., 2010, Hydrothermal alteration in the Reykjanes geothermal system: Insights from Iceland Deep Drilling Program well RN-17: Journal of Volcanology and Geothermal Research, v. 189, p. 172–190, https://doi.org/10.1016/j.jvolgeores.2009.10.018.

McKibben, M.A., and Elders, W.A., 1985, Fe-Zn-Cu-Pb mineralization in the Salton Sea geothermal system, Imperial Valley, California: Economic Geology and the Bulletin of the Society of Economic Geologists, v. 80, p. 539–559, https://doi.org/10.2113/gsecongeo.80.3.539.

Mernagh, T.P., and Mavrogenes, J., 2019, Significance of high temperature fluids and melts in the Grasberg porphyry copper-gold deposit: Chemical Geology, v. 508, p. 210–224, https://doi.org/10.1016/j.chemgeo.2018.09.040.

Óskarsson, F., and Galeczka, I.M., 2017, Reykjanes Production Field Geochemical Monitoring in 2016: Iceland GeoSurvey (ÍSOR) Report 2017/020 for HS Orka, 118 p.

Pettke, T., Oberli, F., Audetat, A., Guillong, M., Simon, A., Hanley, J., and Klemm, L.M., 2012, Recent developments in element concentration and isotope ratio analysis of individual fluid inclusions by laser-ablation single- and multiple-collector ICP–MS: Ore Geology Reviews, v. 44, p. 10–38, https://doi.org/10.1016/j.oregeorev.2011.11.001.

Roedder, E., 1984, Fluid Inclusions: Mineralogical Society of America Reviews in Mineralogy 12, 646 p., https://doi.org/10.1515/9781501508271.

Rottier, B., Kouzmanov, K., Bouvier, A.-S., Baumgartner, L.P., Wälle, M., Rezeau, H., Bendezú, R., and Fontboté, L., 2016, Heterogeneous melt and hypersaline liquid inclusions in shallow porphyry type mineralization as markers of magmatic-hydrothermal transition (Cerro de Pasco District, Peru): Chemical Geology, v. 447, p. 93–116, https://doi.org/10.1016/j.chemgeo.2016.10.032.

Shmulovich, K.I., Tkachenko, S.I., and Plyasunova, N.V., 1995, Phase equilibria in fluid systems at high pressures and temperatures, *in* Shmulovich, K.I., et al., eds., Fluids in the Crust: Equilibrium and Transport Properties: London, Chapman & Hall, p. 193–214, https://doi.org/10.1007/978-94-011-1226-0.

Simon, A.C., Pettke, T., Candela, P.A., Piccolli, P.M., and Heinrich, C.A., 2006, Copper partitioning in a melt-vapour-brine-magnetite-pyrrhotite assemblage: Geochimica et Cosmochimica Acta, v. 70, p. 5583–5600, https://doi.org/10.1016/j.gca.2006.08.045.

Steele-MacInnis, M., Lecumberri-Sanchez, P., and Bodnar, R.J., 2015, Synthetic fluid inclusions XX: Critical *PTX* properties of H_2O-$FeCl_2$ fluids: Geochimica et Cosmochimica Acta, v. 148, p. 50–61, https://doi.org/10.1016/j.gca.2014.09.026.

Zierenberg, R.A., Friðleifsson, G.Ó., Elders, W.A., Schiffman, P., Fowler, A.P.L., and Reed, M., 2021, Active basalt alteration at supercritical conditions in IDDP-2 drill core, Reykjanes, Iceland, *in* Proceedings World Geothermal Congress 2020, 10 p. (in press).

Printed in USA